ELSEVIER

Biochimica et Biophysica Acta 1453 (1999) 161–174

BIOCHIMICA ET BIOPHYSICA ACTA

BBA

Targeted disruption of the mouse ferrochelatase gene producing an exon 10 deletion

Scott T. Magness [a], David A. Brenner [a, b,*]

[a] *Curriculum in Genetics and Molecular Biology, University of North Carolina at Chapel Hill, Chapel Hill, NC 27599-7038, USA*

[b] *Departments of Medicine, Biochemistry and Biophysics, University of North Carolina at Chapel Hill, Chapel Hill, NC 27599-7038, USA*

Received 16 July 1998; received in revised form 15 October 1998; accepted 16 October 1998

Abstract

Protoporphyria is a disease characterized by a deficiency in ferrochelatase, the terminal enzyme in the heme biosynthetic pathway, which catalyzes the chelation of iron and protoporphyrin to form heme. Clinical symptoms arise from an accumulation of protoporphyrin behind the partial enzyme block and include photosensitivity and sometimes hepatobiliary disease. Protoporphyria is described as an dominant disease, yet patients exhibit decreased ferrochelatase activities of 15–30% of normal, not 50% as might be expected. Missense, nonsense, and splicing mutations have been identified in ferrochelatase cDNA from protoporphyric patients. In this study we introduce an exon 10 deletion, an analogous mutation to that described in some protoporphyric patients, into the mouse embryonic stem (ES) cell genome via homologous recombination. Targeted ES cells were confirmed by Southern blot analysis. Expression of wild-type and exon 10-deleted mRNA was demonstrated by reverse transcriptase–polymerase chain reaction (RT–PCR) and cDNA sequencing. Ferrochelatase levels were analyzed by immunoblotting. Ferrochelatase activity was measured by the chelation of zinc and mesoporphyrin, and by the decrease in protoporphyrin accumulation after adding δ-aminolevulinic acid. In the exon 10+/− ES cells there is expression of both wild-type and exon 10-deleted mRNA, a 50% decrease in cross-reactive material with an anti-ferrochelatase antibody, and an approximate 50% decrease in ferrochelatase activity compared to wild-type ES cells. Therefore, an exon 10 deletion alone is insufficient to decrease ferrochelatase activity to the levels in protoporphyric patients. This suggests the requirement of an additional mutation to decrease the expression of the wild-type allele.

Keywords: Protoporphyria; Ferrochelatase; Exon 10 deletion; Embryonic stem cell; Gene targeting

1. Introduction

Ferrochelatase is the final enzyme in the heme biosynthetic pathway and catalyzes the chelation of ferrous iron and protoporphyrin IX to form heme. The human ferrochelatase gene consists of 11 exons which span a region of approximately 40 kb on chromosome 18q21 [1–3]. The ferrochelatase gene is expressed in all cells, which require its product, heme, for essential proteins including the respiratory cytochromes [4,5]. The highest level of ferrochelatase gene expression is in erythroid cells to supply the heme for hemoglobin [6,7].

Protoporphyria (PP) is an inherited disease that is characterized enzymatically by a deficiency in ferro-

* Corresponding author. University of North Carolina at Chapel Hill, CB #7038, Department of Medicine, Chapel Hill, NC 27599-7038, USA. Fax: +1-919-966-7468;
E-mail: dab@med.unc.edu

0925-4439/99/$ – see front matter
PII: S0925-4439(98)00096-9

chelatase activity and biochemically by increased protoporphyrin levels. The clinical symptoms consist of photosensitivity [8] and occasionally hepatobiliary disease [9,10], which can progress to hepatic failure and require liver transplantation [11]. The clinical symptoms arise from the accumulation of the protoporphyrin, which is mainly produced during erythropoiesis [8,12].

Multiple defects in the ferrochelatase gene, which include point mutations, nucleotide deletions, and a partial chromosome deletion [13], have been identified in patients with protoporphyria. The point mutations have resulted in frameshifts and stop codons [14,15], amino acid substitutions [1,16,17], and splicing defects [18–22]. Protoporphyria is generally inherited as an autosomal dominant trait with variable penetrance [23], with each patient or carrier having one mutant ferrochelatase allele and one wild-type (i.e., no detected mutation) allele. On the basis of either having deficient enzymatic activity or of carrying the identified mutation, one parent of each patient has been identified as the carrier of the mutant ferrochelatase allele and one parent as having only wild-type alleles. Rare cases of protoporphyria inherited as a recessive trait have been reported [24–26].

The enzymatic activity of ferrochelatase in protoporphyric patients is usually reported at 15% to 30% of normal, although a 50% reduction of enzymatic activity would be expected in an autosomal dominant disease with a null allele. Three hypotheses have been suggested to explain this less-than-50% activity. One hypothesis is that ferrochelatase is a homodimer such that the mutant ferrochelatase acts as a dominant negative protein to inhibit the wild-type protein [1]. The functional size of ferrochelatase is 82 kDa by radiation inactivation, which is consistent with a functional ferrochelatase dimer [27]. A second hypothesis is that the accumulated protoporphyrin acts to inhibit the enzymatic activity of the active ferrochelatase thereby lowering its apparent maximum velocity further. A third hypothesis is that the 'normal' non-mutant ferrochelatase allele in patients is expressed at a lower level so that the ferrochelatase activity is less than 50% of normal [23]. An A to G polymorphism at position −251 kb (from the start codon) of the ferrochelatase promoter has been identified in some patients with protoporphyria [28]. The functional significance of this polymorphism is unknown, and it is not localized to any of the *cis*-acting elements identified in the promoter [5].

Two animal models have been described for protoporphyria. A natural occurring mutation in cattle requires a homozygous recessive genotype for phenotypic expression [29,30]. Secondly, a mouse mutagenized with EMU (ethylnitrosourea) [31], has been described that contains a T to A transversion at nucleotide 293 [32]. This mutation must exist in a homozygous state to result in a protoporphyric phenotype. Neither of these animal models provides a paradigm of genetic heritability that is similar to that described for dominantly transmitted human protoporphyria.

The extensive sequence data on the ferrochelatase gene that has been generated from protoporphyric patients has led to testable hypotheses on the molecular pathogenesis of this disease. In the present study we have introduced an exon 10 deletion into one ferrochelatase allele by targeting the genome of mouse embryonic stem (ES) cells. This exon 10 deletion is functionally analogous to the exon 10 deletion in ferrochelatase mRNA which has been described for several individuals and families with protoporphyria [19,28]. Exon 10 of ferrochelatase in human and mouse are highly conserved with only a single amino acid change; valine 362 in human [33] is alanine 361 in mouse [4]. When exon 10-deleted human ferrochelatase is expressed in bacteria, the mutant ferrochelatase has no enzymatic activity [34]. The absence of amino acids conferred by exon 10 is thought to disrupt the 2 iron/2 sulfur cluster which is located in the carboxyl terminus and required for ferrochelatase activity [34,35].

If the resultant mutant ferrochelatase protein acts in a dominant negative manner, or if the accumulated protoporphyrin inhibits the enzymatic activity of the wild-type ferrochelatase protein, then we predict the exon 10+/− mutant cell will have a ferrochelatase activity less than 50% of normal. If the function of the wild-type allele is unaffected by the mutant allele, then we predict a ferrochelatase activity of 50% of normal, which is consistent with the requirement of an additional mutation to further reduce the ferrochelatase activity in patients with protoporphyria.

2. Materials and methods

2.1. Targeting vector

The parental targeting vector, OSDUPDEL, contains the neomycin resistance marker for positive selection and the thymidine kinase marker for negative selection. The targeting vector arms derived from regions flanking exon 10 of the mouse ferrochelatase gene were isolated from a cosmid clone containing exons 3–11. The cosmid clone, 2719, was digested with restriction endonucleases and mapped by Southern blot using a ^{32}P-labeled oligo probe specific for the mouse ferrochelatase exon 10. The sequence for the exon-specific probe was deduced from the human intron/exon boundaries. A 10 kb *Eco*RI fragment containing part of intron 8, and exon 9 to 11 was identified, subcloned (clone RID) into pBluescript SK+ (Stratagene, San Diego, CA), and further analyzed by automated sequencing. To preserve the *cis*-elements required for mRNA splicing, we identified two DNA fragments that contained intact splice donor and acceptor sites which would allow exon 9 to be spliced to exon 11. A 4.5 kb *Alw*NI fragment containing part of intron 8, exon 9 and part of intron 9, and a 1.8 kb *Bam*HI fragment containing part of intron 10 and exon 11 was isolated from the RID clone. The ends of both fragments were blunted with Klenow using standard methods [36]. The 6.1 kb fragment was inserted into the *Pml*I site, and the 1.8 kb fragment was inserted into the *Hpa*I site of OSDUPDEL. Orientation of the mouse ferrochelatase gene inserts were assessed by restriction endonuclease analysis and automated sequencing.

2.2. Cell culture and targeting selection

The ES cell clone (BK4), a subclone of E14TG2a, was used for targeting the mouse ferrochelatase gene [37]. The cell line was derived from a 129/Ola mouse strain. ES cells were maintained on irradiated mouse embryonic fibroblasts in DMEM-H, 15% fetal bovine serum (Gibco/BRL, ES qualified), 0.1 mM β-mercaptoethanol, and 2 mM L-glutamine. Approximately 2×10^7 ES cells were electroporated with 15 μg of the mouse ferrochelatase targeting vector linearized with *Pme*I restriction endonuclease. The cells were suspended in 0.5 ml of phosphate-buffered saline (PBS) with the DNA and pulsed in a 4-mm gap electroporation cuvette with 350 V, 50 μF for 1 s. Cells were immediately transferred to a 10-cm plate containing G418-resistant, irradiated embryonic fibroblasts in the growth media previously described. After 24 h, the growth medium was supplemented with 200 μg/ml geneticin (Gibco/BRL, Gaithersburg, MD) and 50 μg/ml ganciclovir. Following 10 days of selection, clonal populations were isolated, expanded and analyzed for proper targeting by Southern blot.

After selection, undifferentiated wild-type and MFC10+/− ES cells were maintained in growth medium supplemented with 4 U/ml rLIF (recombinant leukemia inhibiting factor, Gibco/BRL). To initiate primary differentiation, ES cells were trypsinized, washed twice with PBS, then 1.5×10^5 cells were plated in bacterial grade petri dishes containing Iscove's media supplemented with 15% fetal calf serum (Hyclone, Logan, UT), 1% glutamine 0.2% monothioglutamate (MTG), 50 μg/ml ascorbic acid, 200 μg/ml iron saturated human transferrin and 5% protein-free hybridoma media II (PFHMII, Gibco/BRL). Differentiation cultures were maintained in a humidified atmosphere containing 5% CO_2 at 37°C for 4 days.

2.3. Southern blot analysis and RT–PCR

Individual G418 resistant/ganciclovir sensitive colonies were analyzed for correct targeting by Southern blotting [36]. Genomic DNA was isolated by standard methods [38], digested with *Eco*RI restriction endonuclease, separated on a 0.7% agarose Tris-acetate–EDTA (TAE) gel, transferred to Magnagraph membrane (MSI, Westboro, MA), and UV crosslinked. The blot was probed with an exon 11-specific ^{32}P-labeled random primed probe, which would distinguish between homologous recombination or random integration. After 12 h of hybridization in Rapid-Hyb buffer (Amersham, Arlington Heights, IL) containing 10^6 cpm/ml of probe, the blot was washed once in 5×SSC/0.1%SDS at 55°C, once in 0.1×SSC/0.1% SDS at 55°C, twice in 0.1×SSC/0.1% SDS at 60°C, and then exposed to film (XOMAT-AR, Kodak, Rochester, NY) for 48 h at −80°C with intensifying screens.

RT–PCR was used to analyze the spliced RNA transcript from the targeted allele. Trizol reagent

(Gibco/BRL) was used to isolate total RNA from ES clones that had been separated from embryonic fibroblast feeder cells by passaging 3–4 times in feeder-cell free tissue culture dishes. The culture dishes were treated with 0.1% gelatin in PBS prior to the addition of growth medium and cells. One μg of total RNA was added to a standard RT reaction [36], then 1/5 of the RT reaction (about 120 ng of template) was used for PCR amplification using a primer set that amplified a 340 bp region from exon 8 (PR1: 5′-CCG ACT GGT TTG GCA GTC CA-3′) to exon 11 (PR2: 5′-GAA GGA TTT AGT CTT CCT GCA-3′). Temperatures were cycled 30 times at 94°C for 15 s, 58°C for 15 s, and 72°C for 45 s. Amplification products were analyzed on a 4% TBE–acrylamide gel stained with ethidium bromide.

2.4. Ferrochelatase immunoblot

To assess the ferrochelatase levels in targeted cells, undifferentiated (feeder-cell free) wild-type and MFC10+/− ES cells were lysed in RIPA buffer (0.15M NaCl, 50 mM Tris–HCl (pH 7.2), 1% deoxycholic acid, 1% Triton-X 100, 0.1% SDS) containing 10 μg/ml PMSF. 15 μg of whole cell lysate was separated on a 10% SDS–polyacrylamide gel and electrophoretically transferred to nitrocellulose. Equal loading of protein was assessed by Ponceau S staining. The membrane was then blocked with BLOTTO (5% w/v non-fat dried milk in water) for 15 min at room temperature. Then, a 1:500 dilution in BLOTTO of anti-recombinant human ferrochelatase polyclonal antibody [39] was applied to the blot and allowed to incubate at room temperature for 4 h. The blot was then washed once with BLOTTO and twice in TBS–Tween (Tris-buffered saline containing 0.1% Tween-20). A goat anti-rabbit alkaline phosphatase conjugated secondary antibody (Santa Cruz Biotechnologies, Santa Cruz, CA) was then applied at a 1:1000 dilution in BLOTTO and allowed to incubate for 1 h at room temperature. The membrane was washed once in TBS–Tween, once in BLOTTO and twice in TBS–Tween for 10 min each at room temperature. Western Blue substrate (Promega, Madison, WI) was added and the immunoblot was allowed to develop for approximately 20 min.

2.5. δ-Aminolevulinic acid assay

The δ-aminolevulinic acid (ALA) assay to indirectly assess ferrochelatase activity was performed as previously described [39,40]. Wild-type and MFC10+/− ES cells were plated into 6-well cluster 35-mm tissue culture dishes and allowed to grow to confluency. Cells were washed twice with PBS, and 2.0 ml of fresh DMEM-H growth media (without serum) was added that contained 50 μM $FeSO_4$ and 0, 50, 100, 250, 500 or 750 μM ALA (Porphyrin Products, Logan, UT). Cells were incubated in a humidified atmosphere containing 5% CO_2 at 37°C for 16, 20 and 24 h. After incubation in ALA, the cells were washed once with PBS, and 750 μl of 1:1 (v/v) 0.1 N perchloric acid/methanol solution was added to extract the protoporphyrin. The samples were fluorometrically analyzed for protoporphyrin with protoporphyrin standards (Porphyrin Products) using a Perkin–Elmer LS-50B spectrofluorimeter (excitation: 406 nm; emission: 605 nm).

2.6. Ferrochelatase activity assays

The zinc–protoporphyrin assay was performed essentially as described [39,41]. Approximately 1×10^7 undifferentiated ES cells or embryoid bodies from a 4-day differentiation culture were lysed in palmitic acid buffer (0.25 M Tris–HCl (pH 7.4), 1.75 mM palmitic acid, 1% (v/v) Tween-20) containing 10 μg/ml PMSF. Lysates were sonicated twice in a Branson sonicator for 10 s and incubated on ice. The enzymatic chelation of zinc and protoporphyrin was carried out in a reaction that contained 500 μg of whole cell lysate, 100 μM zinc acetate, and 100 μM protoporphyrin in palmitic acid buffer. The reaction was incubated at 37°C in the dark. After 30 min, 0.5 ml of ice-cold 8:2 methanol/DMSO (dimethyl sulfoxide) was added to stop the reaction. The protein was pelleted before loading the HPLC column by spinning for 10 min at $12\,000\times g$. To detect the zinc–protoporphyrin product, 200 μl of the reaction was applied to a Delta Pak, 5 μm, C_{18} 300 Å, HPLC column (Waters, Milford, MA) and separated in an 88% methanol, 12% 1 M ammonium actetate (pH 5.16) mobile phase with a 1.5 ml/min flow rate. The column flow-through was

directed into the flow cell adapter of the spectrofluorimeter, which was set to an excitation wavelength of 410 nm and an emission wavelength of 590 nm. Concentrations of zinc–protoporphyrin were determined by comparing samples to a standard curve derived from zinc–protoporphyrin (Porphyrin Products).

2.7. Ferrochelatase kinetics

The zinc–mesoporphyrin assay was performed essentially as described [42]. Undifferentiated ES cells were grown to confluency, and washed twice with PBS. Four 10-cm plates were lysed in 250 μl ice-cold sucrose buffer (10 mM Tris-acetate (pH 8.1), 0.25 M sucrose) and freeze-thawed twice. Lysate protein concentrations were determined using BioRad Protein Assay reagent. Then, 200 μg of total cell lysate was added to each reaction containing palmitic acid buffer and the appropriate amounts of zinc and mesoporphyrin. To determine the K_m and V_{max} for ferrochelatase, mesoporphyrin IX (Porphyrin Products, Logan, UT) was varied to final concentrations of 40 μM, 20 μM, 10 μM, 6.7 μM, or 5 μM with a constant zinc acetate concentration of 200 μM. The zinc acetate was also varied with final concentrations of 40 μM, 20 μM, 10 μM, 6.7 μM, or 5 μM with a constant mesoporphyrin IX concentration of 40 μM. The reaction was allowed to proceed for 30 min at 37°C in the dark and was stopped by the addition of ice-cold 30% DMSO/70% methanol. Before loading the reaction product on the HPLC column, the protein was pelleted at $12\,000 \times g$ for 10 min. To detect the Zn-mesoporphyrin reaction product, 200 μl of the reaction was loaded onto an ODS-Hypersil, 5 μm, 250 mm × 4 mm reverse phase column (Hewlett–Packard, Wilmington, DE) and separated in an 88% methanol, 12% 1 M ammonium actetate (pH 5.16) mobile phase with a 1.25 ml/min flow rate. The column flow-through was directed into the flow cell adapter of the spectrofluorimeter, which was set to an excitation wavelength of 403 nm and an emission wavelength of 574 nm. Concentrations of zinc–mesoporphyrin were determined by comparing samples to a standard curve derived from zinc–mesoporphyrin (Porphyrin Products).

3. Results

3.1. Targeting the mouse ferrochelatase gene

A cosmid clone containing exon 3 to exon 11 of the mouse ferrochelatase gene was mapped by restriction endonuclease analysis, Southern blot analysis and automated DNA sequencing. A 10 kb *Eco*RI fragment of the 3′ end of the ferrochelatase gene, which contained part of intron 8 and exon 9 to exon 11, was subcloned into pBluescript SK+ (Stratagene, San Diego, CA). To introduce an exon 10 deletion into the mouse ferrochelatase gene, two fragments, neither containing exon 10, were cloned flanking the neomycin resistance gene marker. One fragment contained part of intron 8, exon 9 and part of intron 9, and the second fragment contained part of intron 10 and part of exon 11 (Fig. 1). This combination of ferrochelatase gene fragments preserves the splice donor site for exon 9 and the acceptor site for exon 11. The product of a homologous recombination between the targeting vector and the ferrochelatase gene would produce a ferrochelatase allele that would lack exon 10, but contain all splice donor and acceptor sites for the correct splicing of exon 9 to exon 11 in the mRNA.

The linearized ferrochelatase targeting vector was electroporated into ES cells derived from the 129/Ola mouse strain. The ES cells were positively selected for homologous recombination and negatively selected for random integration for 10 days. Individual clones were isolated and expanded, and Southern blot analysis was used to analyze the ES clones for proper targeting of the ferrochelatase gene (Fig. 2). The exon 11-specific probe used in the analysis distinguishes between a random integration event and a homologous recombination event. The targeting ratio for this locus was one homologous recombination to four random integrations.

3.2. The targeted allele produces an exon 10-deleted ferrochelatase mRNA

To determine if the targeted allele was producing ferrochelatase mRNA that resulted from the splicing of exon 9 to 11, we isolated total mRNA from wild-

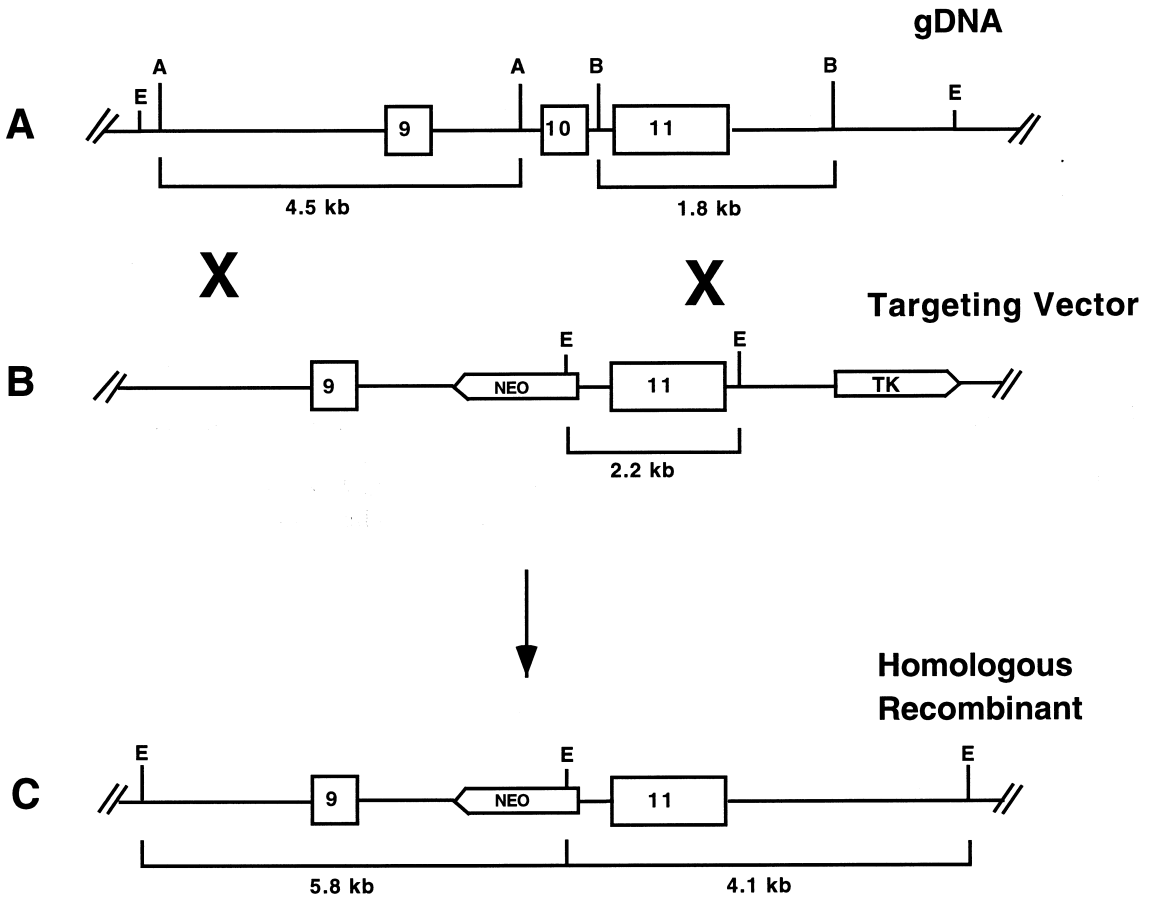

Fig. 1. Targeting the mouse ferrochelatase gene. (A) Schematic of the mouse ferrochelatase locus. Intron regions are represented by lines, exon regions are noted by open boxes. (B) Targeting vector used to introduce an exon 10 deletion into the mouse ferrochelatase gene. The neomycin resistance gene and thymidine kinase gene, and their direction of transcription, are represented by arrowed boxes. (C) The product of a homologous recombination event results in the deletion of exon 10 in the mouse genome. Restriction endonuclease sites are noted: A, *Alw*N;, B, *Bam*HI; E, *Eco*RI.

type and MFC10+/− ES cells (grown in the absence of fibroblast feeders) and analyzed the populations of ferrochelatase mRNA by RT–PCR. The presence of the splice donor site for exon 9 and splice acceptor site for exon 11 should result in the splicing out of the neomycin resistance gene and the joining of exon 9 to 11 to produce an inframe ferrochelatase mRNA without exon 10. RT–PCR analysis of MFC10+/− RNA shows a 340 bp PCR fragment corresponding to the size of the wild-type cDNA and a smaller fragment which corresponds to the exon 10-deleted cDNA (Fig. 3B). A third PCR fragment appears in the RT–PCR amplification of the MFC10+/− RNA (Fig. 3B). The slowest migrating fragment was larger than the wild-type cDNA fragment and was initially thought to contain the neomycin resistance gene cDNA. However, when this band was excised from the gel and re-amplified by PCR, two smaller bands appeared in equivalent quantities that corresponded to the sizes of the wild-type and the exon 10-deleted cDNAs. This suggests that the large PCR fragment is a heteroduplex consisting of a wild-type strand and an exon 10-deleted strand. Mixing equimolar quantities of wild-type and exon 10-deleted single stranded fragments produced a heteroduplex fragment with an equivalent size to that observed in the RT–PCR (not shown). The greater intensity of the wild-type PCR band compared to the exon 10-deleted band was observed in three separate experiments.

To confirm the exon 10-deleted allele was producing an inframe mRNA in which exon 9 was joined to exon 11, the wild-type and exon 10-deleted PCR

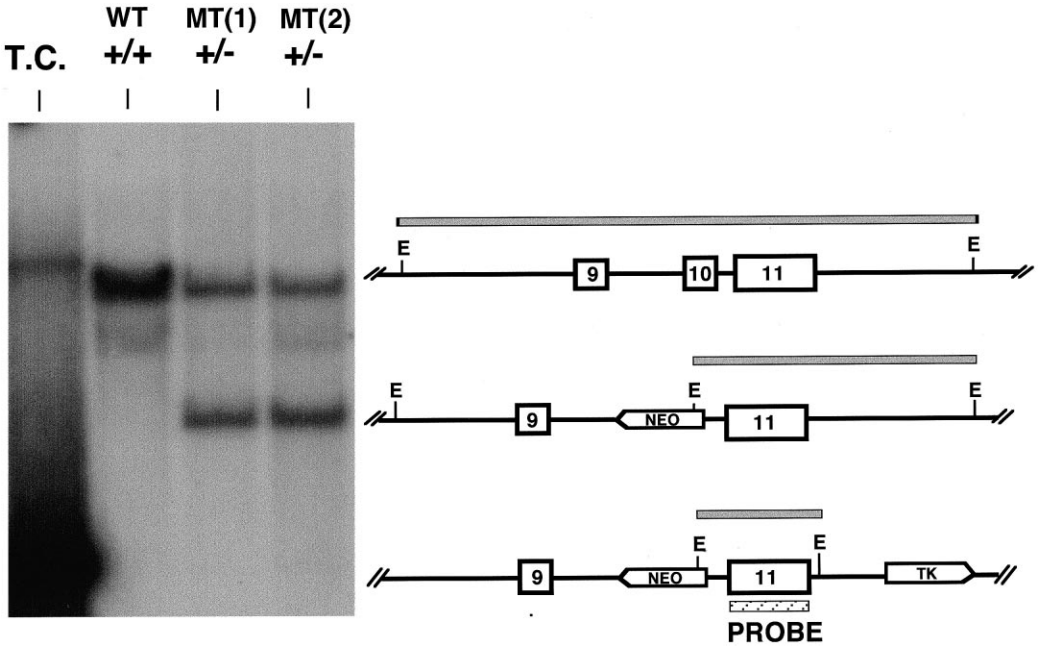

Fig. 2. Southern blot analysis of targeted ES cells. After clonal expansion of geneticin-resistant, ganciclovir-sensitive cells, genomic DNA was isolated, digested with *Eco*RI and analyzed by Southern blot using an exon 11-specific DNA probe (hatched box). T.C. represents the targeting construct, WT represents the parental cell line, and MT(1) and MT(2) represent two individual targeted clones. The schematic to the right of the gel represents the region of each fragment (gray lines) detected by the probe.

fragments were cloned into pPCR II (Invitrogen, Carlsbad, CA) and then analyzed by automated sequencing. The DNA sequence obtained confirms that the PCR fragment amplified from the exon 10-deleted mRNA lacks exon 10 and shows exon 9 sequence adjacent to exon 11 sequence. Translation of this mutant mRNA transcript produces an in-frame ferrochelatase product that lacks the amino acids encoded by exon 10 (Fig. 3C).

3.3. *Accumulation of protoporphyrin in situ is 50% to 60% higher in MFC10+/− cells compared to wild-type cells*

To observe the biochemical manifestation of the exon 10 deletion, we measured the accumulation of protoporphyrin from MFC10+/− and wild-type cells treated with δ-aminolevulinic acid (δ-ALA), the product of the first and rate-limiting enzyme in the heme biosynthetic pathway, δ-ALA synthase. When δ-ALA is added exogenously to cells, it is quickly converted to protoporphyrin by several downstream enzymes, and high levels of protoporphyrin accumulate behind ferrochelatase. As the protoporphyrin is converted to heme, the level of protoporphyrin (measured by fluorescent emission) decreases and provides an indirect measurement of ferrochelatase activity. After treating MFC10+/− or wild-type cells with δ-ALA (from 50 μM to 750 μM), we observed an approximately 50% to 60% higher accumulation of protoporphyrin in MFC10+/− cells compared to wild-type cells (Fig. 4).

3.4. *Ferrochelatase levels and activities in MFC10+/− ES cells are 50% of the wild-type, with a similar K_m for zinc and mesoporphyrin IX*

We next analyzed whole cell extracts for ferrochelatase protein using an anti-human ferrochelatase polyclonal antibody that cross-reacts with mouse ferrochelatase. Immunoblot analysis of undifferentiated wild-type and MFC10+/− ES cells confirms that there is approximately 50% less wild-type ferrochelatase in the MFC10+/− extracts compared to the wild-type extracts (Fig. 5A). We observed no cross-reactive material that would correspond to the size of an exon 10-deleted ferrochelatase.

The activity of ferrochelatase in wild-type and

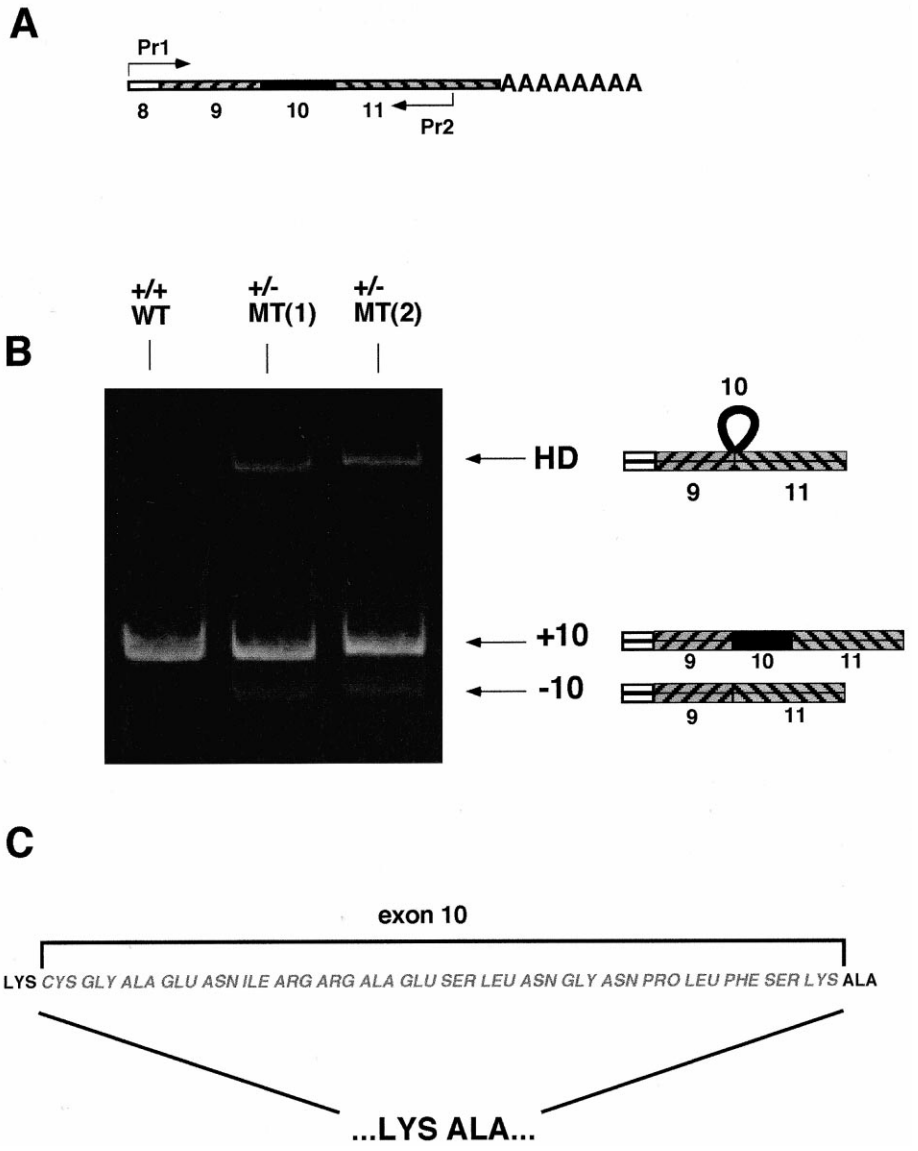

Fig. 3. Expression of the targeted allele. (A) The location of the primers (Pr1 and Pr2) and the region of ferrochelatase mRNA amplified in the RT–PCR reaction. (B) RT–PCR reaction products were separated by PAGE and stained with ethidium bromide for visualization. Schematic to the right of the gel indicates the exon status of the products amplified from the mRNA. +10 contains exon 10, −10 does not contain exon 10. HD represents the heteroduplex that results from the annealing of an exon 10+ and 10− DNA strand. (C) To further confirm the exon 10 status of the PCR bands, +10 and −10 PCR products were cloned and sequenced. The −10 PCR fragment did not contain the sequence for exon 10 (translated sequence in gray), but proved to maintain the proper reading frame for amino acids conferred by exon 9 and exon 11, as demonstrated by the lysine from exon 9 (black) being adjacent to the alanine from exon 11 (black).

MFC10+/− cells was determined by measuring the chelation of ionic zinc and protoporphyrin to make a zinc–protoporphyrin product, which was detected using a sensitive fluorometric assay. Although zinc is not the primary substrate for ferrochelatase in vivo, it is an effective substrate in vitro [42,43]. We assessed the ferrochelatase activity in undifferentiated and 4-day differentiated embryoid bodies of wild-type and MFC10+/− cells. The ferrochelatase activity in the MFC10+/− cells is 40% to 50% lower than in the wild-type cells in both undifferentiated and 4-day differentiated embryoid bodies (Fig. 5B).

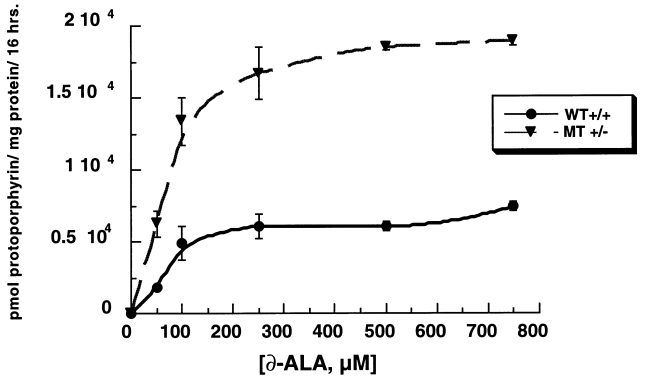

Fig. 4. Increased accumulation of protoporphyrin in MFC10+/− cells. δ-ALA was added to undifferentiated WT and MT (MFC10+/−) ES cells at concentrations that ranged from 50 μM to 750 μM. After 16 h, protoporphyrin was extracted from the cells and analyzed by spectrofluorimetry. Protoporphyrin accumulation is represented as pmol protoporphyrin produced per μg total protein per 16 h. Additional time-course experiments at 20 h and 24 h yielded equivalent results.

To determine if the mutant ferrochelatase was exerting a dominant negative effect on the wild-type ferrochelatase, we assessed the affinity of ferrochelatase for its substrates. We conducted kinetics assays using ferrochelatase activities from whole cell extracts and mesoporphyrin IX as the porphyrin substrate for ferrochelatase, which results in higher assay sensitivity compared to the native protoporphyrin substrate [42]. Zinc was used as the metal substrate to allow for the fluorescent detection of the zinc–mesoporphyrin product. Lineweaver–Burk analysis was used to determine the K_m for the zinc and mesoporphyrin substrates and apparent maximal velocity of the enzyme. Although the maximal velocity for ferrochelatase in the MFC10+/− cells was 48% ± 5% that of wild-type cells, the K_m for mesoporphyrin IX and zinc were similar in both wild-type and mutant cells (K_m mesoporphyrin IX: WT = 4.18 ± 0.60 μM; MFC10+/− = 4.52 ± 0.48 μM; K_m zinc: WT = 11.8 ± 1.3 μM; MFC10+/− = 16.5 ± 1.6 μM) (Fig. 6).

4. Discussion

Protoporphyria is generally described as an autosomal dominant disorder with variable penetrance [23]. Although one would expect that a genetic composition consisting of a normal allele and a null allele for ferrochelatase would result in a 50% decrease in ferrochelatase activity, the activity in protoporphyric patients is consistently only 15% to 30% of normal [9,44,45]. We have introduced an exon 10 deletion, a well described mutation identified in human protoporphyria, into the mouse ferrochelatase gene by homologous recombination to assess the effect of this single mutation on ferrochelatase in undifferentiated and differentiated embryonic stem cells. This study provides new insights into the molecular pathogenesis of protoporphyria.

After targeting the mouse ferrochelatase locus, we assessed the expression from the wild-type and mutated ferrochelatase alleles by RT–PCR analysis, and Western blotting. Using RT–PCR analysis, both wild-type and exon 10-deleted ferrochelatase mRNAs

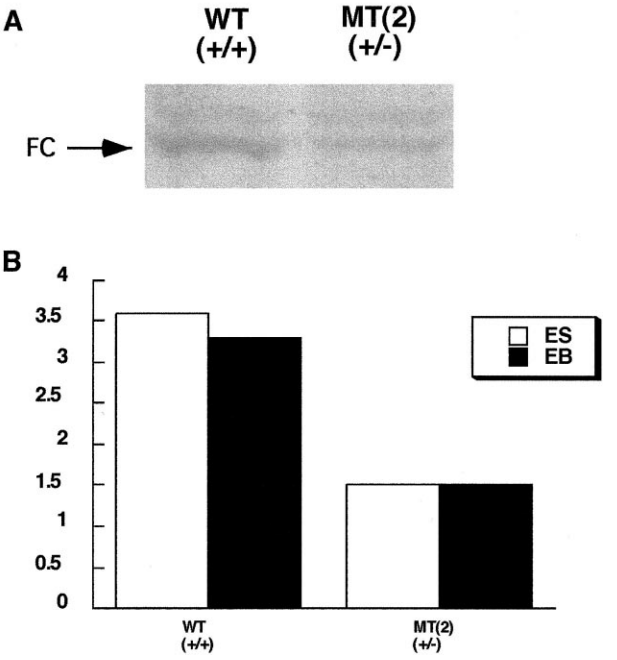

Fig. 5. Ferrochelatase levels and activity in MFC10+/− cells. (A) Fifteen μg of whole cell extracts from undifferentiated WT and MT (MFC10+/−) ES cells were separated by SDS–PAGE and stained with an anti-recombinant human ferrochelatase antibody with subsequent visualization using an alkaline phosphatase conjugated secondary antibody and Western Blue substrate. (B) Ferrochelatase activity from WT and MT cells was assessed by measuring the chelation of zinc and protoporphyrin. The concentration of the zinc–protoporphyrin product was analyzed by HPLC separation and spectrofluorometric detection. White bars represent ferrochelatase activities from undifferentiated ES cells (maintained in rLIF), and black bars represent 4-day differentiated embryoid bodies (EB).

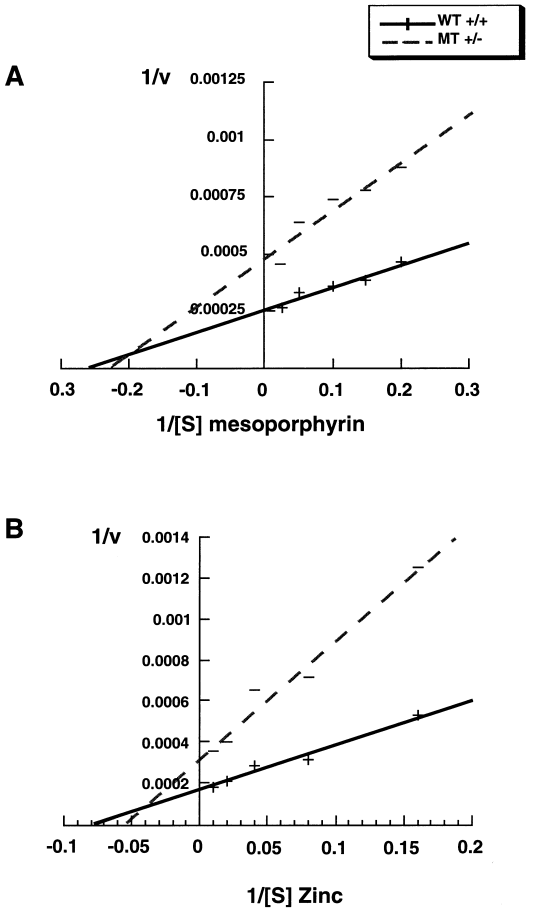

Fig. 6. Kinetic analysis of ferrochelatase from WT or MFC10+/− cells. To determine the V_{max} and K_m for ferrochelatase, (A) mesoporphyrin was varied to a final concentration of 40 μM, 20 μM, 10 μM, 6.7 μM, or 5 μM with a constant zinc concentration of 200 μM, or (B) the zinc was varied to final concentrations of 40 μM, 20 μM, 10 μM, 6.7 μM or 5 μM with a constant mesoporphyrin concentration of 40 μM. The zinc–mesoporphyrin product was separated by HPLC and the concentration subsequently analyzed by spectrofluorimetry. The V_{max} for ferrochelatase in the MFC10+/− cells (MT) was 48% ± 5% of the wild-type (WT) cells. The K_ms for mesoporphyrin were an average of 4.18 μM (WT) and 4.52 μM (MT), and the average K_ms for zinc were 11.8 μM (WT) and 16.5 μM (MT). The data represent average velocities and K_m values from three separate experiments.

from the targeted cells were observed. In three separate experiments using semi-quantitative conditions, the mutant mRNA was expressed at a lower level than that of the wild-type mRNA (Fig. 3B). A recent report assessed ferrochelatase expression from the wild-type allele and the exon 10-deleted allele in a family with protoporphyria [28]. Quantitation of allele specific ferrochelatase expression showed that the exon 10-deleted mRNA levels were less than the wild-type mRNA levels. This decreased mutant ferrochelatase mRNA level may reflect decreased transcription of the mutant allele or decreased mRNA stability. Restriction mapping of the ferrochelatase gene shows that the locus is heterogeneous [46]. Perhaps these genetic differences confer cryptic splice sites which lead to aberrant splicing and instability of the ferrochelatase mRNA. Additionally, studies in other systems have shown that mutations in splicing consensus sites lead to unstable mRNA. For example, a four-base insertion in the coding region of the HEXA gene, which is responsible for Tay–Sachs disease, results in a frameshift and a less stable mRNA [47].

An immunoblot of extracts from exon 10-deleted ES cells using a polyclonal anti-ferrochelatase antibody confirmed approximately 50% less cross-reactive material at 42 kDa compared to extracts from wild-type ES cell (Fig. 5A); however, there was no cross-reactive material observed that corresponded to the size of an exon 10-deficient protein. We and others have analyzed whole cell and mitochondrial extracts from protoporphyric patients with confirmed exon deletions and have been unable to detect any cross-reactive material that would correspond to exon-deleted ferrochelatases [48]. Although we cannot rule out that the polyclonal antibody may not recognize epitopes on the mutant protein, it is more likely that the decreased stability of the mutant mRNA results in less mutant protein which is undetectable using immunostaining methods. Alternatively, it may be a combination of the instability of both the mutant mRNA and mutant protein that results in the inability to detect the exon 10-deleted ferrochelatase.

Although ferrochelatase activities in protoporphyric patients are 15% to 30% of normal, we observed higher ferrochelatase activities of 40% to 50% of normal in both undifferentiated and differentiated exon 10+/− cells. However, there was no difference in ferrochelatase activities in undifferentiated or 4-day differentiated embryoid bodies, which contain various non-erythroid cells and early erythroid precursors. It may be that ferrochelatase is not expressed at higher levels until later in development, or that there were too few erythroid cells expressing high levels of fer-

rochelatase to contribute to an observable increase in activity. Nevertheless, there was a consistent 50–60% decrease in activity observed in undifferentiated and differentiated MFC10+/− cells.

The biochemical manifestation of protoporphyria is the accumulation of protoporphyrin IX. To indirectly measure the ferrochelatase activity in situ, we induced high levels of protoporphyrin production in undifferentiated ES cells by treating cells with δ-ALA, an upstream precursor of protoporphyrin. In the presence of ferrous iron, the protoporphyrin is converted to heme by ferrochelatase and the intracellular levels of protoporphyrin decrease. The observed ferrochelatase activities in the MFC10+/− resulted in the accumulation of 50% to 60% more protoporphyrin compared to wild-type cells. These activity levels are consistent with the in vitro measurements of ferrochelatase activities.

Because ferrochelatase functions as an integral membrane protein, it is conceivable that disruption of membrane composition may affect the activity of the enzyme. Perhaps during erythropoiesis when high levels of lipid soluble protoporphyrin are produced, a protoporphyric cell may accumulate excessive protoporphyrin, which may disrupt the mechanics of the mitochondrial membrane thus decreasing the ferrochelatase activity below 50%. Data from the δ-ALA assay supports this concept by demonstrating a decrease in ferrochelatase activity to 40% to 50% of normal. However, this activity is still greater than the 10% to 27% activity of normal which is observed in fibroblasts from protoporphyric patients using an identical assay [39].

To further examine the possibility that the mutant ferrochelatase may be interacting with the wild-type ferrochelatase to exert a dominant negative effect, we conducted Michaelis–Menten kinetics using extracts from wild-type and MFC10+/− cells. We predicted that if the mutant ferrochelatase was interacting with the wild-type ferrochelatase to disrupt its catalytic activity, then we would observe a V_{max} value of less than 50% in the mutant extracts and an apparent K_m value indicating competitive inhibition. If there was no productive interaction between the two species of ferrochelatase, we would observe a V_{max} of 50% and no change in the apparent K_m. Our data show that there is a 48%±5% decrease in maximal velocity for ferrochelatase in MFC10+/− extracts. The apparent K_m values for zinc and mesoporphyrin are nearly identical for both wild-type and MFC10+/− ferrochelatase, thus corroborating the notion that there is 50% less functional ferrochelatase in the MFC10+/− cells and no dominant negative effect exerted by the exon 10-deleted ferrochelatase. However, since there is a single amino acid difference between human and mouse exon 10, it is conceivable that this difference would prevent the proper dimerization of the mutant and wild-type ferrochelatase monomers, thus there would be no dominant negative effect on the enzyme activity.

Our results suggest that, in addition to a mutation that results in a null allele, a second mutation is necessary to decrease expression of the 'wild-type' allele to produce the protoporphyric phenotype. Recent reports of ferrochelatase levels in protoporphyric patients show that in most cases not only are the ferrochelatase activity levels less than 50%, but so are the ferrochelatase protein levels [48]. It is possible that a mutation in the ferrochelatase promoter could decrease the expression of the wild-type allele. Evidence of the heritability of a low expressing allele has been shown in a family with protoporphyria [28]. Affected individuals possessed a mutant allele that contained an exon 10 deletion, and a wild-type allele that was low expressing. A single polymorphism has been reported in the ferrochelatase promoter, an A to G transition at −251 (from the ATG codon) which is not localized to any described *cis*-acting elements [28]. We are currently investigating the effect of this polymorphism on ferrochelatase gene expression.

Alternatively, aberrant methylation of the CpG island in the ferrochelatase promoter may decrease the expression of the imprinted allele containing the wild-type coding region. In the embryonic rho-globin promoter, hyper-methylation of the 5′ regulatory region results in developmentally regulated suppression of erythroid gene transcription [49], and aberrant methylation of CpG regions are implicated in a disease phenotype in other cases [50]. Studies on the promoter for human O^6-methylguanine DNA methyltransferase gene show that precise nucleosome positioning, which is required for proper expression of the gene, may be influenced by methylation of regions of the CpG islands in the promoter [51]. In this regard, we have shown that appropriate function

of the ferrochelatase promoter requires a chromatin environment [6]. It is tempting to speculate that interaction between proximal and distal *cis*-elements in the ferrochelatase promoter may be regulated by nucleosome positioning, and perhaps parental imprinting of the 'wild-type' allele in protoporphyric individuals results in aberrant nucleosome positioning and a decrease in transcription from this allele.

We cannot discount the possibility that the difference in ferrochelatase activity observed in mouse exon 10-deleted ES cells and human protoporphyric cells may result from species differences. Milder phenotypic expression in gene-targeted mouse models for Duchenne muscular dystrophy [52], neurofibromatosis [53], metachromatic leukodystrophy [54], and cystic fibrosis [55] have been observed. The reason for the less severe clinical sequela of these human mutations in mice is not known. It is proposed that the differences may represent inadequate disruption of the targeted gene, or that there may exist other modulating factors present in humans, and not in mice, that play a role in the phenotypic discordance.

In this study we utilized targeted ES cells grown in culture outside the context of the whole organism. An alternative hypothesis for the discrepancy in activity between the human and mouse exon 10 deletion mutation is that a prolonged exposure to elevated protoporphyrin levels in a patient with protoporphyria may decrease transcriptional or translational expression of the wild-type ferrochelatase allele. It may be that during embryonic development chronic exposure to elevated protoporphyrin levels and/or anemia permanently alter the transcription of genes that are directly, or indirectly, related to ferrochelatase expression. We are currently investigating the effect of this exon 10 deletion in heterozygous mice. Because heme is an indispensable component for many proteins, we predict that a homozygous exon 10 deletion mutation in mice will be lethal.

Acknowledgements

We would like to thank Dr. Harry Dailey (University of Georgia, Athens) for the mouse ferrochelatase cosmid clone, Dr. Oliver Smithies and Dr. Nobuyo Maeda (University of North Carolina, Chapel Hill) for the OSDUPDEL targeting vector and assistance with tissue culture, and the Center for Gastrointestinal and Biological Diseases for computer support. This work was supported by grants DK47361 and DK34987 (D.A.B.).

References

[1] D.A. Brenner, J.M. Didier, F. Frasier, S.R. Christensen, G.A. Evans, H.A. Dailey, A molecular defect in human protoporphyria, Am. J. Hum. Genet. 50 (1992) 1203–1210.
[2] S. Taketani, J. Nazawa, Y. Nakahashi, T. Abe, R. Tokunaga, Structure of the human ferrochelatase gene. Exon/intron gene organization and localization of the gene to chromosome 18, Eur. J. Biochem. 205 (1992) 217–222.
[3] D.M. Whitcomb, N.P. Carter, D.G. Albertson, S.J. Smith, Assignment of the human ferrochelatase gene (FECH) and a locus for protoporphyria to chromosome 18q22., Genomics 11 (1991) 1152–1154.
[4] D.A. Brenner, F. Frasier, Cloning of murine ferrochelatase, Proc. Natl. Acad. Sci. U.S.A. 88 (1991) 849–853.
[5] A.T. Tugores, S.T. Magness, D.A. Brenner, A single promoter directs both housekeeping and erythroid preferential expression of the human ferrochelatase gene, J. Biol. Chem. 269 (1994) 30789–30797.
[6] S.T. Magness, A. Tugores, E.S. Diala, D.A. Brenner, Analysis of the ferrochelatase promoter in transgenic mice, Blood 91 (1998) 320–328.
[7] H. Lake-Bullock, H.A. Dailey, Biphasic ordered induction of heme synthesis in differentiation murine erythroleukemia cells: role of erythroid 5-aminolevulinate synthase, Mol. Cell Biol. 13 (1993) 7122–7132.
[8] M.B. Poh-Fitzpatrick, The 'priming phenomenon' in the acute phototoxicity of erythropoietic protoporphyria, J. Am. Acad. Dermatol. 21 (1989) 311.
[9] J.R. Bloomer, M.J. Phillips, D.L. Davidson, G. Klatskin, Hepatic disease in erythropoietic protoporphyria, Am. J. Med. 58 (1975) 869–882.
[10] J.R. Bloomer, The liver and protoporphyria, Hepatology 8 (1988) 402–407.
[11] J.R. Bloomer, M.K. Weiner, I.C. Bossemaier, D.C. Snover, W.D. Payne, N.L. Ascher, Liver transplantation in a patient with protoporphyria, Gastroenterology 97 (1989) 188–194.
[12] S. Pajovic, V.E. Jones, K.R. Prowse, F.G. Berger, H. Baumann, Species-specific changes in regulatory elements of mouse haptoglobin genes, J. Biol. Chem. 269 (1994) 2215–2224.
[13] S.T. Magness, A. Tugores, S.R. Christensen, C. Wagner-Mcpherson, G.A. Evans, E.W. Naylor, D.A. Brenner, Deletion of the ferrochelatase gene in a patient with protoporphyria, Hum. Mol. Genet. 3 (1994) 1695–1697.
[14] X. Wang, S. Piomelli, M. Peacocke, A.M. Christiano, M.B. Poh-Fitzpatrick, Erythropoietic protoporphyria: four novel frameshift mutations in the ferrochelatase gene, J. Invest. Dermatol. 109 (1997) 688–961.

[15] M. Henriksson, K. Timonen, P. Mustajoki, H. Pihlaja, R. Tenhunen, L. Peltonen, R. Kauppinen, Four novel mutations in the ferrochelatase gene among erythropoietic protoporphyria patients, J. Invest. Dermatol. 106 (1996) 346–350.
[16] S. Imoto, Y. Tanizawa, Y. Sato, K. Kaku, Y. Oka, A novel mutation in the ferrochelatase gene associated with erythropoietic protoporphyria, Br. J. Haematol. 94 (1996) 191–197.
[17] J. Lamoril, S. Boulechfar, H. De Verneuil, B. Grandchamp, Y. Noredmann, J.-C. Deybach, Human erythropoietic protoporphyria: two point mutations in the ferrochelatase gene, Biochem. Biophys. Res. Commun. 181 (1991) 594–599.
[18] Y. Nakahashi, H. Fujita, S. Taketani, N. Ishida, A. Kappas, S. Sassa, The molecular defect of ferrochelatase in a patient with erythropoietic protoporphyria, Proc. Natl. Acad. Sci. U.S.A. 89 (1992) 281–285.
[19] R.P. Sarkany, D.M. Whitcombe, T.M. Cox, Molecular characterization of a ferrochelatase gene defect causing anomalous RNA splicing in erythropoietic protoporphyria, J. Invest. Dermatol. 102 (1994) 481–484.
[20] Y. Nakahashi, H. Miyazaki, Y. Kadota, Y. Naitoh, K. Inoue, M. Yamamoto, N. Hayashi, S. Taketani, Human erythropoietic protoporphyria: identification of a mutation at the splice donor site of intron 7 causing exon 7 skipping of the ferrochelatase gene, Hum. Mol. Genet. 2 (1993) 1069–1070.
[21] Y. Nakahashi, H. Miyazaki, Y. Kadota, Y. Niatoh, K. Inoue, M. Yamamoto, N. Hayashi, S. Taketani, Molecular defect in human erythropoietic protoporpyria with fatal liver failure, Hum. Genet. 91 (1993) 303–306.
[22] X. Wang, M. Poh-Fitzpatrick, S. Tekaetani, T. Chen, S. Piomelli, Screening for ferrochelatase mutations: molecular heterogeneity of erythropoietic protoporphyria, Biochim. Biophys. Acta 1225 (1994) 187–190.
[23] L.N. Went, E.C. Klasen, Genetic aspects of erythropoietic protoporphyria, Ann. Hum. Genet. 48 (1984) 105–117.
[24] J.C. Deyback, V. Dasilva, Y. Pasquier, Y. Nordman, Ferrochelatase in Human Erythropoietic Protoporphyria: The First Case of a Homozygous Form of the Enzyme Deficiency, John Libbey Erotest, 1986.
[25] R.P. Sarkany, G.J. Alexander, T.M. Cox, Recessive inheritance of erythropoietic protoporphyria with liver failure, Lancet 343 (1994) 1394–1396.
[26] X. Schneider-Yin, S. Taketani, B. Schafer, E.I. Minder, Recessive inheritance of erythropoietic protoporphyria with liver failure, Lancet 344 (1994) 337.
[27] J.G. Straka, J.R. Bloomer, E.S. Kempner, The functional size of ferrochelatase determined in situ by radiation inactivation, J. Biol. Chem. 266 (1991) 24637–24641.
[28] L. Gouya, J.C. Deybach, J. Lamoril, V. Da Silva, C. Beaumont, B. Grandchamp, Y. Nordmann, Modulation of the phenotype in dominant erythropoietic, Am. J. Hum. Genet. 58 (1996) 292–299.
[29] G.R. Ruth, S. Schwartz, B. Stephenson, Bovine protoporphyria: The first non-human model of this hereditary photosensitizing disease, Science 198 (1977) 199–201.
[30] J.R. Bloomer, K.O. Morton, R.J. Reuter, G.R. Ruth, Bovine protoporphyria: Documentation of autosomal recessive inheritance and comparison with the human disease through measurement of heme synthase activity, Am. J. Hum. Genet. 34 (1982) 322–330.
[31] S. Tutois, X. Montagutelli, V. Da Silva, H. Jouault, P. Rouyer-Fessard, K. Leroy-Viard, J.L. Guenet, Y. Nordmann, Y. Beuzard, J.C. Deybach, Erythropoietic protoporphyria in the house mouse. A recessive inherited ferrochelatase deficiency with anemia, photosensitivity, and liver disease, J. Clin. Invest. 88 (1991) 1730–1736.
[32] S. Boulechfar, J. Lamoril, X. Montagutelli, J.L. Guenet, J.C. Deybach, Y. Nordmann, H. Dailey, B. Grandchamp, H. de Verneuil, Ferrochelatase structural mutant (Fechm1Pas) in the house mouse, Genomics 16 (1993) 645–648.
[33] Y. Nakahashi, S. Teketani, M. Okuda, K. Inoue, R. Tokunaga, Molecular cloning and sequence analysis of cDNA encoding human ferrochelatase, Biochem. Biophys. Res. Commun. 2 (1990) 748–755.
[34] V.M. Sellers, T.A. Dailey, H.A. Dailey, Examination of ferrochelatase mutations that cause erythropoietic protoporphyria, Blood 91 (1998) 3980–3985.
[35] V.M. Sellers, M.K. Johnson, H.A. Dailey, Function of the [2Fe-2S] cluster in mammalian ferrochelatase: a possible role as a nitric oxide sensor, Biochemistry 35 (1996) 2699–2704.
[36] J. Sambrook, E.F. Fritsch, T. Maniatis, Molecular Cloning: A Laboratory Manual, 2nd ed., Cold Spring Harbor Laboratory Press, Cold Spring Harbor, NY, 1989.
[37] S.K. Bronson, E.G. Plaehn, K.D. Kluckman, J.R. Hagaman, N. Maeda, O. Smithies, Single-copy transgenic mice with chosen-site integration, Proc. Natl. Acad. Sci. U.S.A. 93 (1996) 9067–9072.
[38] B. Hogan, F. Costantini, E. Lacy, Manipulating the Mouse Embryo: A Laboratory Manual, Cold Spring Harbor Laboratory, Cold Spring Harbor, NY, 1986.
[39] S.T. Magness, D.A. Brenner, Ferrochelatase cDNA delivered by adenoviral vector corrects biochemical deficiency in protoporphyric cells, Hum. Gene Ther. 6 (1995) 1285–1290.
[40] J.R. Bloomer, D.A. Brenner, M.J. Mahoney, Study of factors causing excess protoporphyrin accumulation in cultured skin fibroblasts from patients with protoporphyria, J. Clin. Invest. 60 (1977) 1354–1361.
[41] R. Guo, C.K. Lim, T.J. Peters, High-performance liquid chromatographic assays for protoporphyrinogen oxidase and ferrochelatase in human leukocytes, J. Chromatogr. 566 (1991) 383–396.
[42] F.M. Li, C.K. Lim, T.J. Peters, An HPLC assay for rat liver ferrochelatase activity, Biomed. Chromatogr. 2 (1987) 164–168.
[43] G. Goerz, S. Bunselmeyer, K. Bolsen, N.Y. Schurer, Ferrochelatase activities in patients with erythropoietic protoporphyria and their families, Br. J. Dermatol. 134 (1996) 880–885.
[44] J.R. Bloomer, H.L. Bronkowsky, P.S. Ebert, M.J. Mahoney, Inheritance in protoporphyria, Lancet 1 (1976) 226–228.
[45] D.J. Todd, Erythropoietic protoporphyria, Br. J. Dermatol. 131 (1994) 751–766.
[46] L.T. Ostasiewicz, J.L. Huang, X. Wang, S. Piomelli, M.B.

Poh-Fitzpatrick, Human protoporphyria: genetic heterogeneity at the ferrochelatase locus, Photodermatol. Photoimmunol. Photomed. 11 (1995) 18–21.

[47] D.J. Boles, R.L. Proia, The molecular basis of HEXA mRNA deficiency caused by the most common Tay–Sachs disease mutation, Am. J. Hum. Genet. 56 (1995) 716–724.

[48] J. Bloomer, C. Bruzzone, L. Zhu, Y. Scarlett, S. Magness, D. Brenner, Molecular defects in ferrochelatase in patients with protoporphyria requiring liver transplantation, J. Clin. Invest. 102 (1998) 107–114.

[49] R. Singal, R. Ferris, J.A. Little, S.Z. Wang, G.D. Ginder, Methylation of the minimal promoter of an embryonic globin gene silences transcription in primary erythroid cells, Proc. Natl. Acad. Sci. U.S.A. 94 (1997) 13724–13729.

[50] D.N. Mancini, D.I. Rodenhiser, P.J. Ainsworth, F.P. O'Malley, S.M. Singh, W. Xing, T.K. Archer, CpG methylation within the 5′ regulatory region of the BRCA1 gene is tumor specific and includes a putative CREB binding site, Oncogene 16 (1998) 1161–1169.

[51] S.A. Patel, D.M. Graunke, R.O. Pieper, Aberrant silencing of the CpG island-containing human O^6-methylguanine DNA methyltransferase gene is associated with the loss of nucleosome-like positioning, Mol. Cell. Biol. 17 (1997) 5813–5822.

[52] E. Araki, K. Nakamura, K. Nakao, S. Kameya, O. Kobayashi, I. Nonaka, T. Kobayashi, M. Katsuki, Targeted disruption of exon 52 in the mouse dystrophin gene induced muscle degeneration similar to that observed in Duchenne muscular dystrophy, Biochem. Biophys. Res. Commun. 238 (1997) 492–497.

[53] T. Jacks, T.S. Shih, E.M. Schmitt, R.T. Bronson, A. Bernards, R.A. Weinberg, Tumour predisposition in mice heterozygous for a targeted mutation in Nf1, Nat. Genet. 7 (1994) 353–361.

[54] V. Gieselmann, U. Matzner, B. Hess, R. Lullmann-Rauch, R. Coenen, D. Hartmann, R. D'Hooge, P. DeDeyn, G. Nagels, Metachromatic leukodystrophy: molecular genetics and an animal model, J. Inherit. Metab. Dis. 21 (1998) 564–574.

[55] W.K. O'Neal, P. Hasty, P.B. McCray Jr., B. Casey, J. Rivera-Perez, M.J. Welsh, A.L. Beaudet, A. Bradley, A severe phenotype in mice with a duplication of exon 3 in the cystic fibrosis locus, Hum. Mol. Genet. 2 (1993) 1561–1569.